Supporting information

A correlation of the hydrogen evolution reaction activity to the number of defects formed by the decomposition of doped phosphorus species in carbon nanotubes

AI Jie   LIU Zi-wu*   SUN Mao-mao   LIU Ling   WANG Quan-de*

Key Laboratory of Coal-based CO_2 Capture and geological Storage, Jiangsu Province, School of Chemical Engineering and Jiangsu Province Engineering Laboratory of High Efficient Energy Storage Technology and Equipments, China University of Mining and Technology, Xuzhou 221008, Jiangsu, China

E-mail: lzwmsy@cumt.edu.cn,   306088995@qq.com

Electrode preparation and electrochemical experiments

Electrochemical experiments were conducted at room temperature in a three-electrode cell connected to an electrochemical analyzer. PDCNTs1, PDCNTs2, PDCNTs3, PDCNTs4 or Pt-C was coated onto the surface of glassy carbon electrode (5.0 mm in diameter) and used as the working electrode with a loading of 0.458 mg cm^{-2}, an Ag/AgCl with saturated KCl as reference electrode, and a graphite electrode as counter electrode. All potentials were measured and reported vs the potential of Ag/AgCl electrode and converted to reversible hydrogen electrode (RHE) potentials by the Nernst equation: E (RHE) = E (Ag/AgCl) + 0.059 × pH + 0.198. The linear sweep voltammetry (LSV) measurements were performed in the nitrogen-saturated 0.5 mol L^{-1} H_2SO_4 solution at a scan rate of 10 mV s^{-1} and a rotate speed of

1600 r min^{-1}.

Materials Characterization

The morphologies of prepared samples were characterized by the scanning electron microscopy (SEM, ZEISS Merlin), transmission electron microscopy (TEM, Talos F200S). Surface elements were determined by XPS measurements on a Thermo Scientific ESCALAB 250XI using Al $K\alpha$ radiation with the externally contaminated carbon C1s at 284.8 eV as a reference. Crystallinity and defects of catalysts were recorded with a Brucker Raman Spectroscopy Senterra at a wavelength of 532 nm.
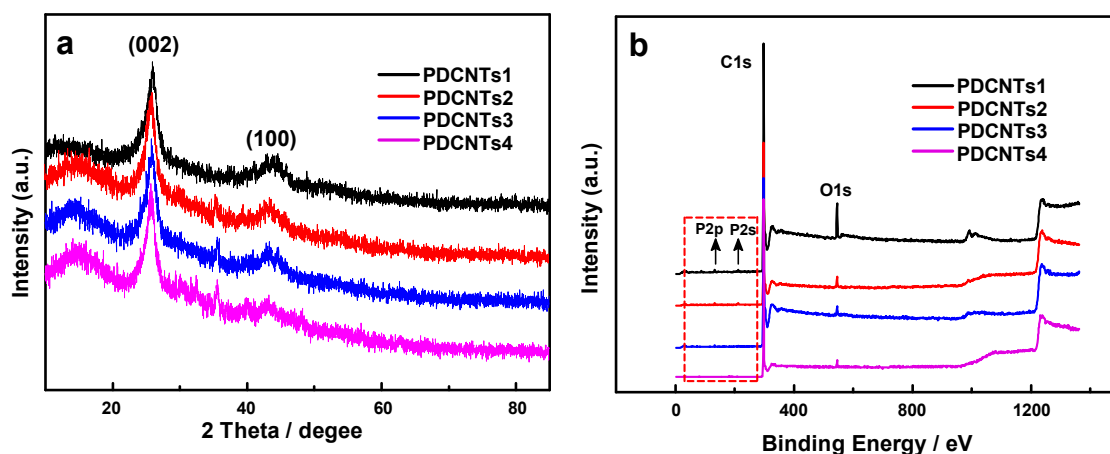

Fig. S1 XRD (a) and X-ray photoelectron spectroscopy (XPS) (b) spectra of PDCNTs1, PDCNTs2, PDCNTs3 and PDCNTs4.
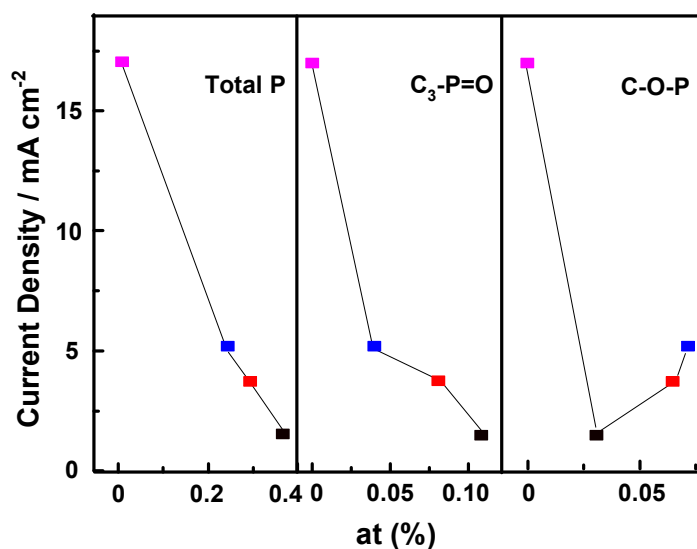
Fig. S2 The dependences of HER current densities (at 0.3 V overpotential) of PDCNTs1 (■), PDCNTs2 (■), PDCNTs3 (■), PDCNTs4 (■) on the total P, C_3-P=O and C-O-P contents.

Geometry optimization, frequency analysis and single-point energy calculation were performed by using the UM062X/6-31G (d, p) functional implemented in the Gaussian 09 software. The binding energy is defined as the energy of the optimized PO-GRO complex minus the energy of corresponding GRO structure and single H^+/OH^- [S1].
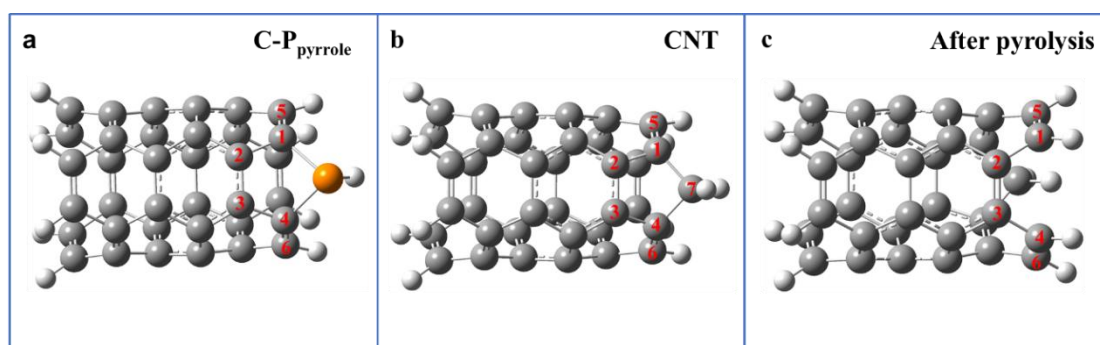

Fig. S3 The CNTs with a C_2-P pyrrole-like configuration (a) the blank normal CNT framework (b) and the corresponding structure (c) after the decomposition of C_2-P species.

Table S1 The charge and spin densities of carbon atoms in the new formed structure after the decomposition of C_2-P pyrrole-like configuration and those of corresponding carbon atoms in the blank.

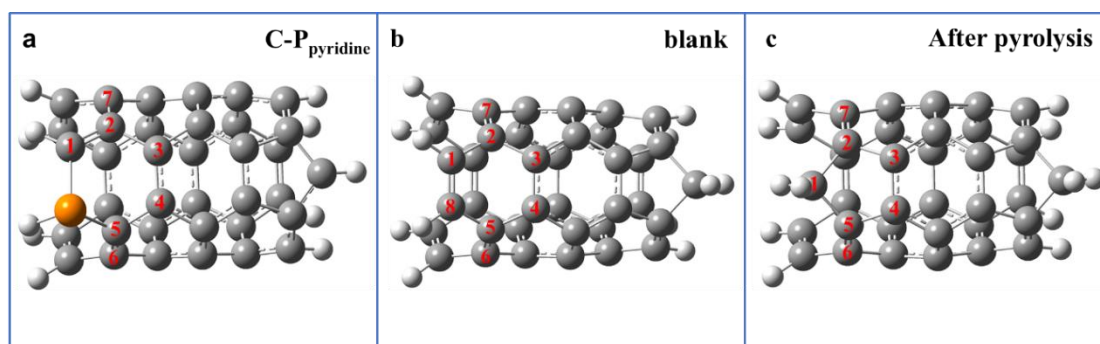| Atom number	Charge density (blank)	Spin density (blank)	Charge density (after pyrolysis)	Spin density (after pyrolysis)
1	0.035	0	-0.125	0
2	-0.014	0	-0.015	0
3	-0.014	0	-0.016	0
4	0.035	0	-0.125	0
5	-0.153	0	-0.140	0
6	-0.153	0	-0.140	0
7	-0.285	0	-	-

Fig. S4 The CNTs with a C_2-P pyridine-like configuration (a) the blank normal CNT framework (b) and the corresponding defect structure (c) after the decomposition of C_2-P species.

Table S2 The charge and spin densities of carbon atoms in the new formed structure after the decomposition of C_2-P pyridine-like configuration and those of corresponding carbon atoms in the blank.

Atom number	Charge density (blank)	Spin density (blank)	Charge density (after pyrolysis)	Spin density (after pyrolysis)
1	-0.123	0	-0.272	0
2	-0.009	0	0.007	0
3	0	0	-0.002	0
4	0	0	-0.002	0
5	-0.009	0	0.007	0
6	-0.021	0	-0.029	0
7	-0.021	0	-0.029	0
8	-0.123	0	-	-

Table S3 The HER TOF values on the bases of the currents and C-P group losses with the C-P content in PDGLs1 as reference.

Samples	n	J	TOF
PDCNTs1	-	1.58×10^{-3}	-
PDCNTs2	0.43×10^{-8}	3.79×10^{-3}	0.69
PDCNTs3	0.52×10^{-8}	5.14×10^{-3}	1.02
PDCNTs4	1.39×10^{-8}	17.21×10^{-3}	1.26

Turnover frequency (TOF) $(s^{-1})= \frac{JA}{2nF}$, where J (A cm^{-2}) is the current density for samples at 0.3 V overpotential, n (mol) is the mole number of C-P group loss with the C-P content in PDGLs1 as reference, A is the geometrical surface area of the glassy carbon electrode (0.1963495 cm^{-2}), F is the faraday constant (96485.3 s A mol^{-1}).

References

[S1] Liu Z W, Shi Q Q, Zhang R F, Wang Q D, Kang G J, Peng F. Phosphorus-doped carbon nanotubes supported low Pt loading catalyst for the oxygen reduction reaction in acidic fuel cells [J]. J. Power Sources 2014, 268: 171-175.